

# Theta-gamma dysrhythmia and auditory phantom perception

## Case report

**DIRK DE RIDDER, M.D., PH.D.,<sup>1–3</sup> ELSA VAN DER LOO, M.Sc.,<sup>1–3</sup>  
SVEN VANNESTE, M.Sc., M.A.,<sup>1–3</sup> STEFFEN GAIS, PH.D.,<sup>4</sup> MARK PLAZIER, M.D.,<sup>1–3</sup>  
SILVIA KOVACS, M.Sc.,<sup>5</sup> STEFAN SUNAERT, M.D., PH.D.,<sup>5</sup> TOMAS MENOVSKY, M.D., PH.D.,<sup>1–3</sup>  
AND PAUL VAN DE HEYNING, M.D., PH.D.<sup>1,2,6</sup>**

<sup>1</sup>Brai<sup>2</sup>n, <sup>2</sup>Tinnitus Research Initiative, <sup>3</sup>Department of Neurosurgery, and <sup>6</sup>Department of ENT, University Hospital Antwerp; <sup>5</sup>Department of Radiology, University Hospital Leuven, Belgium; and <sup>4</sup>General and Experimental Psychology, Ludwig-Maximilians-Universität München, Germany

Tinnitus is considered an auditory phantom percept analogous to phantom pain. Thalamocortical dysrhythmia has been proposed as a possible pathophysiological mechanism for both tinnitus and pain. Thalamocortical dysrhythmia refers to a persistent pathological resting state theta-gamma coupling that is spatially localized at an area where normally alpha oscillations predominate. Auditory cortex stimulation via implanted electrodes has been developed to treat tinnitus, targeting an area of activation on functional MR imaging elicited by tinnitus-matched sound presentation. The authors describe a case in which clinical improvement was correlated with changes in intracranial recordings. Maximal tinnitus suppression was obtained by current delivery exactly at the blood oxygen level–dependent activation hotspot, which colocalizes with increased gamma and theta activity, in contrast to the other electrode poles, which demonstrated a normal alpha peak. These spectral changes normalized when stimulation induced tinnitus suppression, both on electrode and source-localized electroencephalography recordings. These data suggest that theta-gamma coupling as proposed by the thalamocortical dysrhythmia model might be causally related to a conscious auditory phantom percept. (DOI: 10.3171/2010.11.JNS10335)

**KEY WORDS** • auditory cortex • functional magnetic resonance imaging • neurostimulation • tinnitus • thalamocortical dysrhythmia • gamma-band activity • theta-gamma dysrhythmia

**T**INNITUS is a symptom that affects 10%–15% of the population,<sup>1,26</sup> for which no proven treatments exist.<sup>21</sup> It severely impairs the quality of life in 2%–3% of the population,<sup>1</sup> leading to insomnia,<sup>10</sup> anxiety,<sup>3,64</sup> and depression.<sup>3,20</sup>

The most common form of tinnitus, nonpulsatile tinnitus, is considered to be an auditory phantom phenomenon<sup>28</sup> analogous to central neuropathic pain.<sup>42,60</sup> Both disorders share similarities in their clinical expression, pathophysiological mechanisms, and treatment approaches.<sup>12,42,60</sup>

It has been demonstrated that both magnetic<sup>14,31,32,39</sup> and electrical stimulation of the auditory cortex in humans via implanted electrodes<sup>12,14,17,24,56</sup> can benefit patients suffering from tinnitus. Magnetoencephalography

studies in humans with tinnitus have shown a shift of the auditory cortical frequency map at the site of the tinnitus frequency, and the shift is related to the strength of the tinnitus.<sup>43</sup> Other MEG studies have demonstrated that tinnitus is not only related to reorganization of the auditory cortex but also to increased gamma-band activity in the contralateral auditory cortex.<sup>38,63</sup> Furthermore, the amount of reorganization correlates with the tinnitus severity,<sup>43</sup> and the amount of contralateral gamma-band activity correlates with the perceived intensity of the phantom sound.<sup>61</sup> It has been shown that the auditory cortex BOLD signal on fMR imaging correlates with gamma-band firing rate and local field potentials,<sup>44,45</sup> suggesting that fMR imaging can be used as an indirect way of looking at the neural code of tinnitus. Based on further MEG data, thalamocortical dysrhythmia has been proposed as a pathophysiological model for the development of gamma-band activity related to the tinnitus percept.<sup>38</sup> According to this model, tinnitus is caused by an abnormal, spontaneous, and constant gamma-band activity

*Abbreviations used in this paper:* BOLD = blood oxygen level–dependent; dBHL = decibels hearing level; dBSL = decibels sensation level; EEG = electroencephalography; fMR = functional MR; iEEG = intracranial EEG; IPG = internal pulse generator; MEG = magnetoencephalography; sLORETA = standardized low-resolution brain electromagnetic tomography; TMS = transcranial magnetic stimulation; VAS = visual analog scale.

This article contains some figures that are displayed in color online but in black and white in the print edition.

(> 30 Hz) generated as a consequence of hyperpolarization of specific thalamic nuclei; in this case, the medial geniculate body. In normal circumstances, auditory stimuli increase thalamocortical alpha oscillations to gamma-band activity.<sup>9,29</sup> In the deafferented tinnitus state, however, oscillatory alpha activity decreases<sup>40</sup> to theta-band activity (4–7 Hz).<sup>58</sup> As a result, lateral inhibition is reduced, inducing a surrounding gamma-band activity known as the “edge effect.”<sup>37,38</sup> Synchronized gamma-band activity in the auditory cortex is proposed to bind auditory events into 1 coherent conscious auditory percept.<sup>9,29,35,36,52,59</sup> Thus, decreased lateral inhibition in the auditory cortex results in increased gamma-band activity, a prerequisite for auditory consciousness, and therefore possibly contributing to the perception of a phantom sound.

A recent MEG study demonstrated that secondary auditory cortex stimulation for contralateral tinnitus suppression does interfere with the neural signatures of thalamocortical dysrhythmia, and suggested that auditory cortex stimulation may be effective if areas exhibiting abnormal, dysrhythmic activity are targeted.<sup>51</sup> In the present study, an electrode was implanted on an area overlying the posterior superior temporal gyrus, more specifically at the area of BOLD activation elicited by tinnitus frequency-specific sound presentation. Postoperative recordings were performed on the extradurally implanted electrodes, and power/frequency analyses were used to look for signs of (thalamo)cortical dysrhythmia, that is, theta-gamma dysrhythmia, and to correlate these findings with the area of BOLD activation and the area of maximal tinnitus suppression, respectively.

### Case Report

**History.** This 36-year-old Colombian man presented at the multidisciplinary Tinnitus Research Initiative Clinic of the University Hospital Antwerp, Belgium, with a 14-year history of intractable bilateral pure tone tinnitus. The tinnitus scored 9 of 10 on a VAS, and was bothersome enough for this Colombian patient to seek help in faraway Belgium. Previous treatments consisted of medication (flunarizine, ginkgo biloba, carbamazepine, sertraline, alprazolam, gabapentine, topamirate), acupuncture, low-level laser therapy, and TMS.

**Audiological Test.** A small hearing deficit between 4000 and 6000 Hz in both ears was confirmed by pure tone audiometry. Hearing thresholds for the other frequencies were within normal limits. Tinnitus matching in a soundproof booth specified the pure tone to 4000 Hz, 20 dB SL. Tinnitus matching in the MR imaging unit environment correlated more to a phantom sound perception at 6000 Hz.

**Acquisition of fMR Images.** Functional MR imaging can accurately visualize auditory activity in patients with tinnitus,<sup>33</sup> and the BOLD response differs in the auditory cortex between patients with tinnitus and controls,<sup>57</sup> suggesting that it can visualize areas involved in the generation of the tinnitus percept.

Functional MR imaging of the auditory cortex performed in a way previously described (by music presen-

tation;<sup>33,57</sup> see Fig. 1A), as well as using tinnitus-matched sound (6000 Hz; see Fig. 1B), demonstrated an asymmetry in activation and deactivation strength at the primary and secondary auditory cortex. Deactivations were elicited that were nonoverlapping with activations and with a more widespread anatomical distribution (Fig. 1B, *green area*).

**Transcranial Magnetic Stimulation.** This procedure, performed in tonic mode<sup>18</sup> at 1 Hz, and centered over the right secondary auditory cortex, suppresses tinnitus bilaterally by 70% in a placebo-controlled way. The TMS results could be reproduced on 2 separate occasions. The TMS of the right auditory cortex in burst mode<sup>15,16</sup> improved tinnitus bilaterally by 90%, with a residual inhibition for 15 minutes, also in a placebo-controlled way.

**Operation.** The electrode was implanted using a technique that has been previously described.<sup>12–14</sup> The Lamitrode 44 lead is made of 16 electrodes with a 28-mm electrode span and a 60-cm lead length, configured with 2 offset rows of 4 electrodes, each 4 × 2.5 mm, with 3-mm spacing between the electrodes. A straight 8-cm-long incision is made overlying the auditory cortex, as determined by the fMR imaging-guided neuronavigation. The 8 × 2-cm craniotomy and the location for the electrode placement are tailored in the same fMR imaging-based navigated fashion. After bipolar coagulation of the dura mater to inactivate potential sensory nerve endings that can cause pain on electrical stimulation, the lead, placed extradurally, is sutured to the dura and tunneled subcutaneously to the abdomen, where it is externalized.

**Postoperative Course.** The postoperative course was uneventful. One hour after completion of the operation (with the IPG still in “off” mode), the patient woke up with the same tinnitus as before the operation. A postoperative CT scan of the electrodes was obtained and was fused with preoperative fMR images to verify correct positioning of the electrode.

The patient was discharged on the 1st postoperative day and returned on the consecutive days for further testing and programming. The programming was performed by a technician who had not seen the fused postoperative CT and fMR imaging study and was executed in a bipolar fashion by trial and error, asking the patient on each programming trial whether the tinnitus improved or not. Finally a program was elected, with the IPG set to deliver impulses with a duration of 0.5 msec and a rate of 6 pulses per second and 2.0 mA, resulting in a 95% tinnitus suppression bilaterally. The stimulation was turned off for 5 seconds and on for 5 seconds, with only 1 pole positive and 1 pole negative; the other 6 poles were not activated. Placebo stimulation with the same electrode configuration was not successful in inducing tinnitus suppression. The poles that yield maximal tinnitus suppression on electrical pulse delivery colocalize with the area of BOLD response (Fig. 2A). Recordings of the iEEG data were performed using the implanted electrode when tinnitus perception was high (VAS Score 8 of 10) and during residual inhibition periods after stimulation when tinnitus perception was low (VAS Score 1 of 10). During

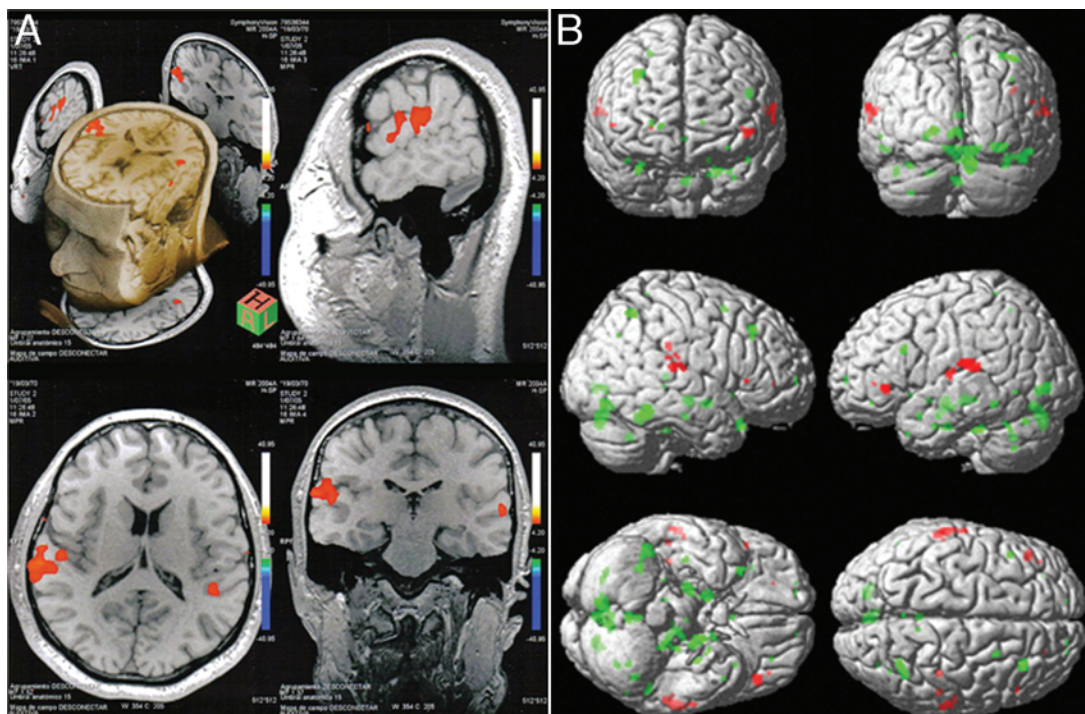


**FIG. 1.** **A:** Functional MR images with 3D reconstruction demonstrating areas of BOLD activation (red) obtained by music presentation. **B:** The 3D reconstructions of BOLD activation (red) and deactivation (green) areas obtained by tinnitus-matched sound (6000 Hz) ( $p < 0.05$ , corrected for multiple comparisons).

high tinnitus perception, the spectral analysis of the bipolar derivation of the electrode contacts shows a normal alpha peak, except for the contacts overlying the BOLD activation area (corresponding to the contacts of maximal stimulation efficacy).<sup>47</sup> At this location, a predominant theta peak is noted, a peak that disappears when tinnitus perception is low (Fig. 3). Increased gamma-band activity is also noted, as well as a dip in 50-Hz activity related to the notch filter (Fig. 3). Correlations in spectral amplitudes are very high for frequencies ranging from 10 to 45 Hz for electrode contacts overlying the BOLD activation hotspot, with gamma range frequencies correlating with frequencies in the delta and theta range. Contacts more remote from the BOLD activation hotspot show lower correlations overall and no correlations between the gamma frequencies and the lower frequencies (Fig. 5).

After 1 week, the patient returned home and has remained almost free of tinnitus ever since (a period of 3 years), with a VAS score of 1 of 10, the tinnitus being perceived only when the patients concentrates on hearing it. The patient reports a small temporary increase in the perceived tinnitus intensity (to 2 or 3 of 10) when he is feeling sick or extremely tired.

Postoperative sLORETA EEG studies demonstrated that the stimulation decreased the amount of gamma activity in the stimulated auditory cortex concomitant with improving tinnitus intensity scores (Fig. 6). Furthermore, functional connectivity analysis (sLORETA connectivity, <http://www.uzh.ch/keyinst/loreta.htm>) associated functional theta connectivity changes with improving tinnitus (Fig. 7).

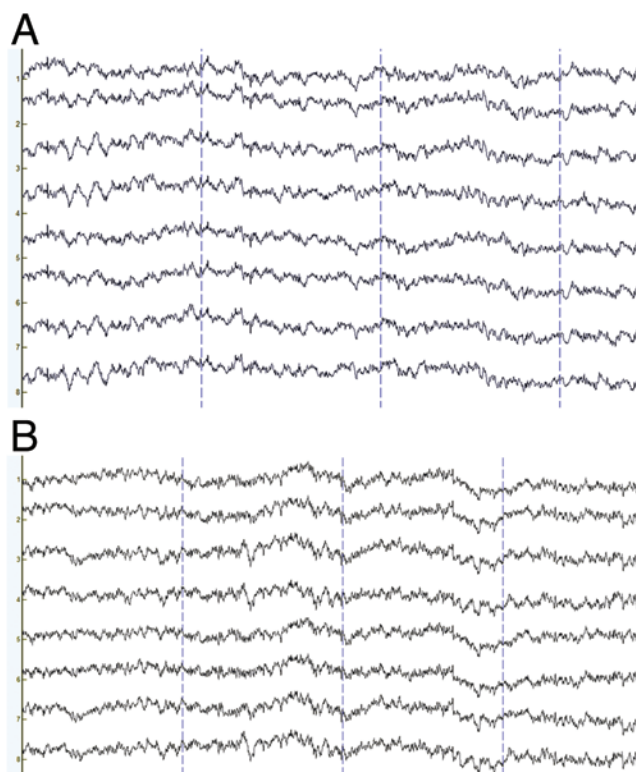


**FIG. 2.** Electroencephalography tracings obtained under the 2 tinnitus conditions. **A:** Approximately 5 days after implantation, VAS Score 8; the "tinnitus present" condition. **B:** At VAS Score 1; very low tinnitus perception.



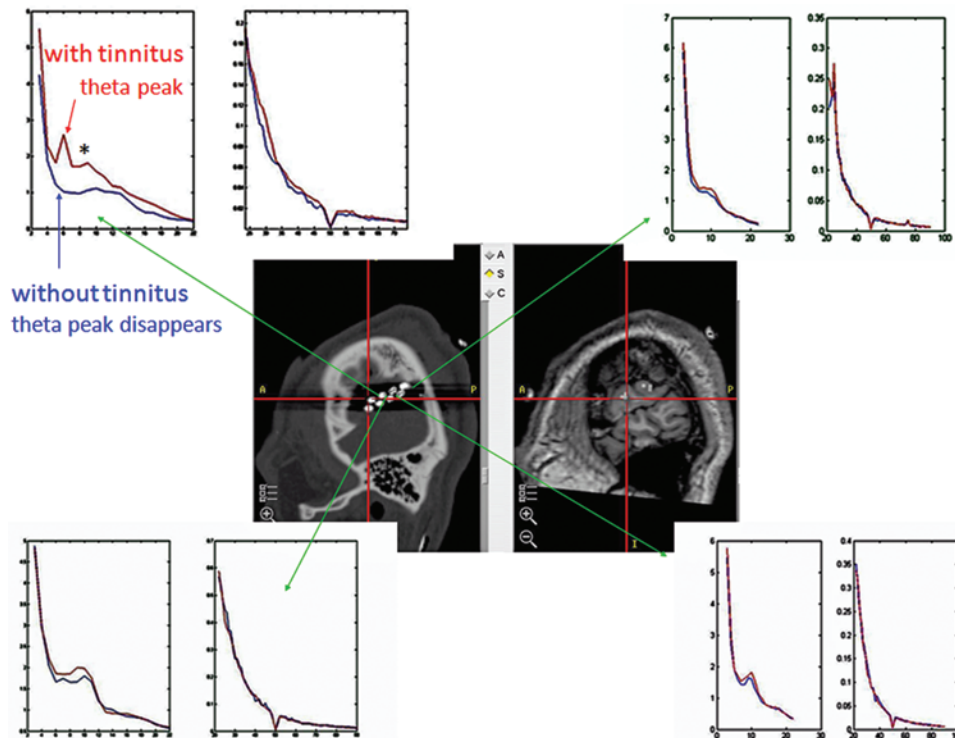


**FIG. 3.** **Center:** Preimplantation fMRI image fused with postimplantation CT scan. The BOLD activation hotspot corresponds to the bipolar derivation of electrodes 1 and 5 (anterior poles) of the implanted electrode. Power-frequency plots in 4 quadrants are shown. **Upper Left:** Bipolar recordings of BOLD activation area during a period of loud tinnitus (VAS Score 8 of 10) and of little to no tinnitus (VAS Score 1 of 10). Note that the theta peak on the anterior electrodes is present only during the tinnitus percept (*upper curve*) and absent during the “no tinnitus” recordings (*lower curve*) (during a period of residual inhibition). The 3 other power-frequency plots only demonstrate a normal alpha peak around 10 Hz and a 50-Hz dip due to a notch filter. *Asterisk* denotes the alpha peak. **Upper Right:** Readings from the most posterior poles. **Lower Left:** Readings from anterior to mid-pole, adjacent to the BOLD activation area. **Lower Right:** Readings from the midposterior poles, adjacent to most the posterior bipolar recordings. Scale of x axis of the **upper left** and **lower left** plots starts at 2 Hz at the x-y intersection and increases by 2 Hz; thus, the theta peak is at 6 Hz.

### Description of Examination Techniques

**Pure Tone Audiometry.** Pure tone audiometry was performed in this patient using the “up 5–down 10” method at 0.125, 0.25, 0.5, 1, 2, 3, 4, 6, and 8 kHz.<sup>6</sup> The mean hearing loss was computed afterward by taking the mean

auditory threshold at 0.5, 1, 2, 4, and 8 kHz. The audiogram slope was computed by subtraction of the mean threshold between 0.5 and 1 kHz and the mean threshold between 4 and 8 kHz.

In patients with tinnitus, the highest frequency-specific threshold between both ears was taken into account. The tinnitus analysis was performed contralateral to the

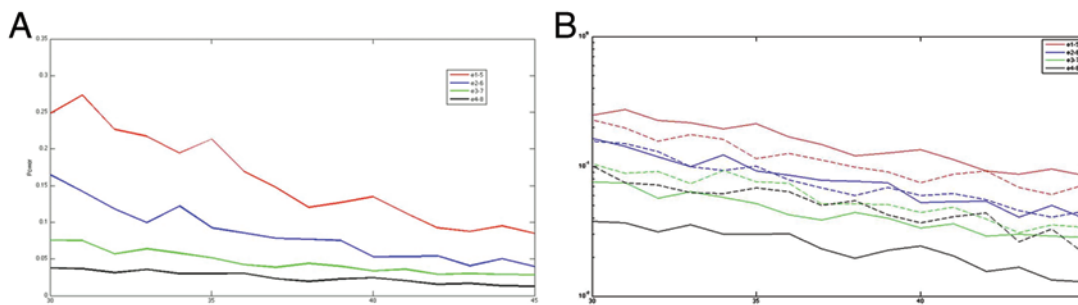


**FIG. 4.** Power spectra of bipolar derivations computed between adjacent electrode contacts estimated by multitaper fast Fourier transform for gamma frequencies (30–45 Hz). **A:** The *red lines* represent the spectral power of the contacts overlying the BOLD activation hotspot on fMRI imaging. Maximal gamma power is noted underlying the BOLD activation area, with a progressive decrease related to increasing distance from the BOLD area. **B:** The *solid lines* represent the “tinnitus present” condition (VAS Score 8), whereas the *dashed lines* represent the condition with very low tinnitus perception (VAS Score 1). Gamma-band activity decreases when tinnitus intensity decreases.



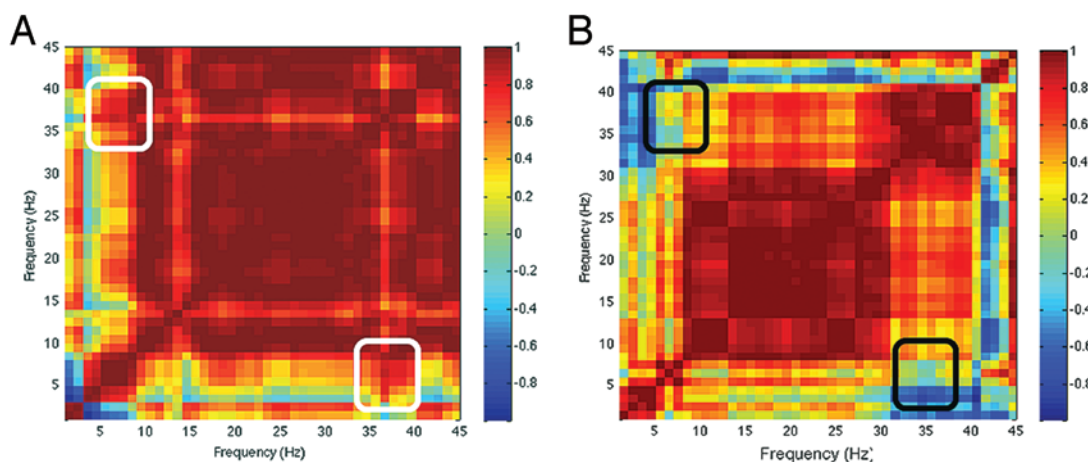


**Fig. 5.** Correlation plots of power spectra for the different electrodes. **A:** Electrode contacts overlying the BOLD activation hotspot (Contacts 1, 2, 5, and 6). **B:** Electrode contacts more remote from the BOLD activation hotspot (Contacts 3, 4, 7, and 8). Unipolar derivations with reference near the vertex were used, to ensure sufficient contacts to yield a correlation. Correlations in spectral amplitudes are very high for frequencies ranging from 10 to 45 Hz, for electrode contacts overlying the BOLD activation hotspot, with gamma range frequencies correlating with frequencies in the theta range (*white squares in A*). Contacts more remote from the BOLD activation hotspot show lower correlations overall and no correlations between the gamma and theta frequencies (*black squares in B*).

ear with the worst tinnitus. The analysis consisted of an assessment of frequency and intensity. The tinnitus intensity (dBSL) was computed by subtracting the absolute tinnitus intensity (dBHL) with the auditory threshold at that frequency.

**Procedure for fMR Imaging Examination.** In a block design, 50 seconds of tinnitus frequency-specific sound (delivered at 90 dB to both ears simultaneously) was presented, alternating with 50 seconds of nonstimulation. This alternation was repeated 6 times.

**Imaging Parameters.** The patient underwent imaging on a 3-T MR machine (INTERA; Philips Medical Systems, Inc.) with a 6-channel phased-array dedicated head coil. For functional imaging, a T2\*-weighted, gradient echo, echo planar imaging sequence was used, with a TE of 33 msec and a TR of 5000 msec (acquisition matrix  $80 \times 80$ , field of view  $230 \times 230$  mm). We used a clustered volume acquisition technique, in which the acquisition time was shorter than the TR, namely 2000 msec, leaving

a 3000-msec silent gap between each echo planar imaging volume acquisition. A sensitivity encoding reduction factor of 2.5 was used.

For anatomical reference, a high-resolution 3D T1-weighted turbo field echo was used, with a TE/TR of 4.60/9.70 msec and an acquired voxel size of  $0.98 \times 0.98 \times 1.20$  mm<sup>3</sup> (acquisition matrix  $256 \times 256$ , field of view  $250 \times 250$  mm<sup>2</sup>, sensitivity encoding reduction factor 3; 128 turbo field echo shots).

**Analysis of fMR Imaging Data.** Postprocessing was performed with SPM99 software and consisted of realignment (to correct for bulk head motion), coregistration of the functional and structural images, spatial smoothing, and statistical analysis to determine significantly activated brain regions ( $p < 0.05$ , corrected for multiple comparisons).

**Preimplantation fMR Imaging and Postimplantation CT Fusion.** The preimplantation, high-resolution, T1-weighted MR image; the preimplantation fMR image;

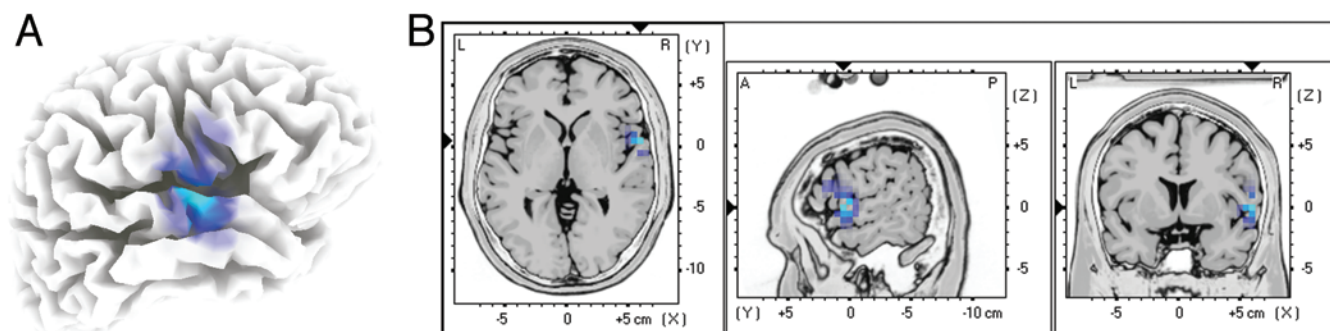


**Fig. 6.** Comparison of tinnitus-related gamma-band activity in the stimulated auditory cortex 5 days after surgery (VAS Score 4) and 2.5 years after electrode implantation (VAS Score 0–1) on source-analyzed EEG studies (sLORETA, <http://www.uzh.ch/keyinst/loreta.htm>). *Blue* indicates less gamma activity after stimulation. Panel **A** is a 3D view, and **B** shows axial, sagittal, and coronal sLORETA EEG slices.

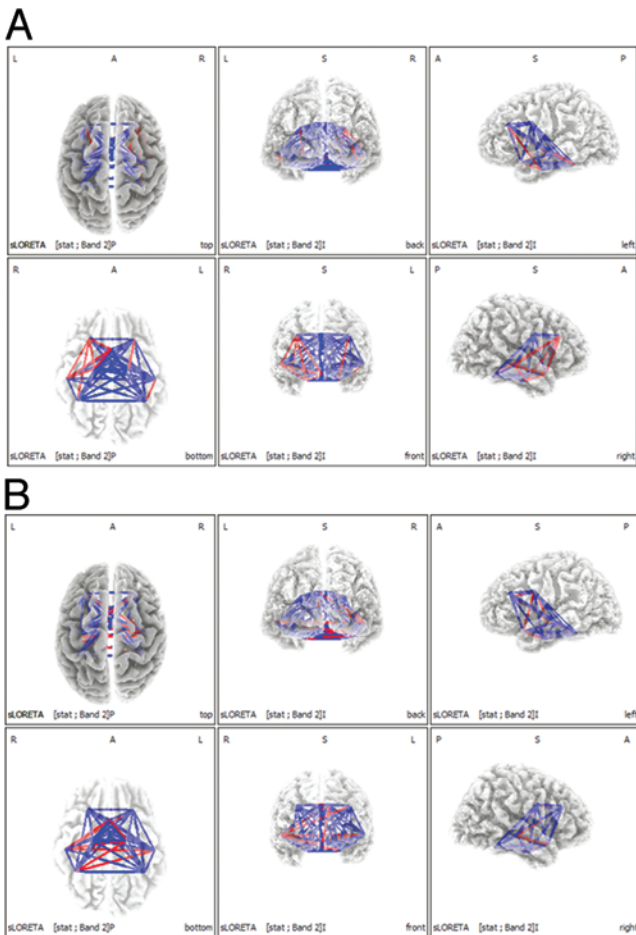


**FIG. 7.** **A:** Comparison of connectivity (sLORETA connectivity, <http://www.uzh.ch/keyinst/loreta.htm>) approximately 5 days after implantation for theta activity (4–7.5 Hz) between VAS scores of 4 and 0–1. *Blue lines* indicate more connectivity on VAS Score 4, whereas the *red lines* indicate more connectivity on VAS Score 0–1. **B:** Comparison of connectivity (sLORETA connectivity, <http://www.uzh.ch/keyinst/loreta.htm>) between approximately 1 month and 2.5 years after implantation for theta activity (4–7.5 Hz). *Blue lines* indicate more connectivity after 1 month of implantation, whereas the *red lines* indicate more connectivity after 2.5 years of implantation.

and the postimplantation CT scan were fused in 2 different ways. One fusion was performed in the Stealth neuronavigation system (Stealth; Medtronic, Inc.) (Fig. 3). For correlations with intracranial recordings, fusions were performed with CURY software (Neuroscan; Compumedics Ltd.), allowing us to visualize the intracranial poles overlying the fMR imaging hotspot (Fig. 4).

**Transcranial Magnetic Stimulation.** The TMS, performed with a figure-eight coil, was applied twice in a placebo-controlled way, using a Super Rapid stimulator (Magstim, Inc.) that is capable of repetitive pulse modes of up to 50 Hz. The procedure is performed as follows: before the TMS session, the patient grades the tinnitus on a VAS. The motor threshold to TMS is first determined by placing the coil over the motor cortex. The intensity of the magnetic stimulation is slowly increased until a clear contraction is observed in the contralateral first dorsal in-

terosseous muscle. The coil is then moved to a location over the left and right auditory cortex in separate sessions (5–6 cm above the entrance of the external auditory meatus on a straight line to the vertex). With the intensity of the stimulation set at 90% of the motor threshold, the site of maximal tinnitus suppression is determined using 1-Hz stimulation. When tinnitus suppression is noted, the patient is asked to estimate the decrease in tinnitus as a percentage, according to the VAS. The procedure is repeated with stimulations at 5, 10, and 20 Hz, each session consisting of 200 pulses. When tinnitus suppression is induced by TMS, the patient is asked to notify the technician when the tinnitus returns to baseline before the next TMS frequency is applied. Burst stimulation is performed in a similar fashion. Bursts are presented at 5, 10, and 20 Hz, with 3 and 5 high-frequency (50-Hz) pulses, respectively, in each burst. Both tonic and burst TMSs are applied.<sup>15,16</sup> Different frequencies and intensities are applied at both sites.

**Electrode Implantation.** Two days after the last TMS, an extradural octopolar electrode (Lamitrode 44; St. Jude Medical, Neuromodulation Division) was implanted overlying the right secondary auditory cortex for extradural electrical stimulation. The Lamitrode 44 lead is made of 8 electrodes, with a 28-mm electrode span and a 60-cm lead length, configured with 2 offset rows of 4 electrodes, each 4 × 2.5 mm, with 3-mm spacing between the electrodes. A straight 6-cm-long incision was made overlying the auditory cortex, as determined by fMR imaging-guided neuronavigation. The 6 × 2-cm craniotomy and the location for the electrode placement were tailored in the same navigated fashion. The lead, which was extradurally placed after coagulation of the dura mater to prevent stimulation-induced dural pain, was sutured to the dura. It was tunneled subcutaneously to the abdomen and connected to the IPG (Genesis; ANS Inc.), which was implanted in a subcutaneous pocket in the abdomen.

**Intracranial EEG.** Recordings of iEEG data were performed continuously on all 8 electrode contacts during a period of high tinnitus perception (VAS Score 8 of 10) and a period of low tinnitus perception (VAS Score 1 of 10). The recording of low tinnitus perception was obtained during the inhibitory period following cortical stimulation (sampling rate 1000 Hz, bandpass 1–130 Hz, referenced to Cz). Impedances of intracranial contacts and scalp reference remained below 5 kΩ.

**Analysis of iEEG Data.** Electrodes were rereferenced to an adjacent electrode contact in the opposite row, giving 4 bipolar derivations formed by Contacts 1 and 5, 2 and 6, 3 and 7, and 4 and 8 (Fig. 3). All analyses were done in Matlab (The Mathworks) using EEGLAB, an open source toolbox for processing electrophysiological data (<http://scn.ucsd.edu/eeqlab/index.html>) and the Fieldtrip open source toolbox (<http://www.ru.nl/fcdonders/fieldtrip/>). Data were preprocessed by dividing the continuously recorded iEEG data into epochs of 1 second. Epochs with artifacts were removed.

**Frequency Analysis.** The spectral analysis of the bipolar derivations computed between opposing electrode

contacts were estimated with the aid of multitaper fast Fourier transform<sup>41</sup> using 3 tapers. This approach provides a way to smooth the spectra in the frequency domain, allowing better control of higher-frequency oscillatory components. In addition, correlation plots between spectral amplitudes at discrete frequencies for electrode contacts overlying the fMR BOLD activation hotspot and for contacts not overlying this area were computed while tinnitus perception was high. Because bipolar computations yield only 4 derivations, we chose to use unipolar derivations (with a reference near the vertex). This allowed us to compare the correlation in amplitudes between different frequencies for poles: 1, 2, 5, and 6 for the BOLD activation hotspot and 3, 4, 7, and 8 for “far” poles (those farther away from the hotspot).

**Collection of EEG Data.** The EEG studies were obtained in a fully lighted room with the patient sitting upright in a small chair. The actual testing took approximately 5 minutes. The EEG data were sampled with 19 electrodes (Fp1, Fp2, F7, F3, Fz, F4, F8, T7, C3, Cz, C4, T8, P7, P3, Pz, P4, P8, O1, and O2) in the standard 10/20 International placement and referenced to linked ears. Data were collected with the patient’s eyes closed (sampling rate 1024 Hz, bandpass 0.15–200 Hz). Impedances were checked to remain below 5 k $\Omega$ . Data were resampled to 128 Hz, bandpass filtered to 2–44 Hz, and subsequently transposed into Eureka! Software (version 3.0; freeware available at [www.NovaTechEEG](http://www.NovaTechEEG)) to be plotted and carefully inspected for manual rejection of artifacts. All episodic artifacts, including eye blinks, eye movements, teeth clenching, body movement, or electrocardiography artifacts, were removed from the stream of the EEG recording.

**Source Localization.** The mean power in delta (2–3.5 Hz), theta (4–7.5 Hz), alpha1 (8–9.5 Hz), alpha2 (10–12.5 Hz), beta1 (13–18 Hz), beta2 (18.5–21 Hz), beta3 (21.5–30 Hz), and gamma (30.5–45 Hz) bands was calculated. The sLORETA modality was used to estimate the intracerebral electrical sources that generated the scalp-recorded activity in each of the 8 frequency bands.<sup>50</sup> The sLORETA modality computes electric neuronal activity as current density (A/m<sup>2</sup>) without assuming a predefined number of active sources. The sLORETA solution space consists of 6239 voxels (voxel size 5 × 5 × 5 mm) and is restricted to cortical gray matter and hippocampi, as defined by the digitized MNI (Montreal Neurological Institute) 152 template.<sup>25</sup> Scalp electrode coordinates on the MNI brain are derived from the 10/5 International system.<sup>30</sup>

**Connectivity.** Coherence and phase synchronization between time series corresponding to different spatial locations are usually interpreted as indicators of the so-called connectivity. However, any measure of dependence is highly contaminated, with an instantaneous, nonphysiological contribution due to volume conduction and low spatial resolution (see Pascual-Marqui<sup>49</sup>). Therefore, Pascual-Marqui<sup>48</sup> introduced a new technique (that is, Hermitian covariance matrices) that removes this confounding factor to a great extent. This measure of dependence can be applied to any number of brain areas jointly, that is, to

distributed cortical networks. The activity of these networks can be estimated with sLORETA. The sLORETA modality was used to estimate the intercerebral electrical sources that generated the scalp-recorded activity in each of the 8 frequency bands.<sup>50</sup>

Measures of linear dependence (coherence) between the multivariate time series are defined. The measures are expressed as the sum of lagged dependence and instantaneous dependence. The measures are nonnegative, taking the value 0 only when there is independence of the pertinent type, and are defined in the frequency domain: delta (2–3.5 Hz), theta (4–7.5 Hz), alpha1 (8–9.5 Hz), alpha2 (10–12.5 Hz), beta1 (13–18 Hz), beta2 (18.5–21 Hz), beta3 (21.5–30 Hz), and gamma (30.5–45 Hz). Based on this principle, lagged linear connectivity was calculated. Regions of interest were defined based on previous brain research on tinnitus.

## Discussion

For the auditory phantom to be suppressed, the current applied via the electrodes has to arrive at the auditory cortex. It is unknown whether the primary or secondary auditory cortex is the main generator of the tinnitus intensity.<sup>61</sup> The current is actually targeted at the BOLD signal changes on the lateral posterior part of the superior temporal gyrus, that is, at the secondary auditory cortex, and it is assumed that it modulates activity in the primary auditory cortex via functional connections that exist between the lateral posterior superior temporal gyrus and the primary auditory cortex on the Heschl gyrus, buried deep inside the posterior part of the sylvian fissure. That this stimulation can modulate the primary auditory cortex has been argued by our experience with a single case in which an fMR imaging session was performed without stimulation (with tinnitus) and after stimulation during a period of residual inhibition, that is, tinnitus intensity modulation.<sup>27</sup> This case study demonstrated no changes in the secondary auditory area directly underlying the electrode, but in the primary auditory area in the Heschl gyrus.

Because the electrode is placed extradurally and the craniotomized bone is repositioned and fixed with titanium plates, the electrode volume decreases the distance between stimulating poles and the lateral part of the posterior superior temporal gyrus, similarly to what has been described for spinal cord stimulation.<sup>46</sup>

During programming, the stimulation is initiated at 1 mA, with the pulse width fixed at 300  $\mu$ sec, and increased until an improvement is noted by the patient. Once the patient experiences a difference in the tinnitus percept, the amplitude, pulse width, and frequency are adjusted by increasing and decreasing the individual parameters to what yields best suppression of the phantom percept. Because the patient does not feel whether the stimulation is on or off, this can be easily done in a placebo-controlled way.

For an auditory stimulus to be consciously perceived, activation of the primary auditory cortex is a prerequisite but is not sufficient. Studies performed in patients in a vegetative state who do not have conscious auditory per-



cepts reveal that auditory stimuli still activate the primary auditory cortex but that there is no functional connectivity to frontal areas in these patients.<sup>4,5,19,34</sup> The global workspace model suggests that conscious perception of sensory events requires activation of sensory cortex embedded in a cortical network called the global workspace, which extends beyond the primary sensory regions, including prefrontal, parietal, and cingulate cortices.<sup>19</sup> Indeed, a recent study analyzing differences in long-range coupling between patients with tinnitus and controls show altered activity in the central auditory system, with alterations in so-called alpha and gamma networks including frontal, parietal, and cingulate brain areas for patients with tinnitus.<sup>55</sup> Based on the developments in network science such as scale-free network models,<sup>2,7,22</sup> brain areas with many functional ingoing and outgoing connections, also called hubs, can be retrieved in the brain of a patient with tinnitus,<sup>54</sup> demonstrating that the neural generator of tinnitus is not phrenologically limited to the auditory cortex but is more likely to be an emerging property related to a complex adaptive network in the brain.

Thalamocortical dysrhythmia has been proposed as a pathophysiological model for the generation of tinnitus. It predicts that both theta- and gamma-band activity can be recorded in patients suffering tinnitus, but not in the moment when patients do not perceive tinnitus. Whole-head EEG might not have the spatial resolution to do this and might be limited in its value for recording high frequencies due to muscle artifact. Recordings from extradurally implanted electrodes are less prone to artifacts and yield higher spatial resolution.

The patient underwent implantation of an electrode overlying the secondary auditory cortex on the posterior superior temporal gyrus. In accordance with recent reports demonstrating that gamma-band local field potentials from the auditory cortex correlate with the BOLD signal,<sup>44,45</sup> maximal gamma-band activity in this patient colocalizes with the area of BOLD activation generated by tinnitus frequency-specific sound presentation in the MR imaging unit, suggesting that the BOLD activation area localizes the generator of the tinnitus accurately.

If so, electrophysiological signs of thalamocortical theta-gamma dysrhythmia have to be retrieved at the area of BOLD activation. Indeed, only at the area of BOLD activation are the theta and gamma bands increased, a phenomenon associated with a decrease of alpha activity, during periods of tinnitus perception in comparison with periods of no tinnitus perception. From the correlation plots, it also appears that, during tinnitus perception, gamma-band activity in the area overlying the BOLD activation hotspot is coupled more to theta than more distantly from the BOLD activation area, suggesting that thalamocortical theta-gamma dysrhythmia is present only at the BOLD activation hotspot. It has been suggested that theta activity synchronizes large spatial domains and binds together specific assemblies by the appropriate timing of higher-frequency localized oscillations<sup>8,23,62</sup> and that higher-frequency gamma oscillations are confined to a small neuronal space, whereas very large networks are recruited during slow oscillations.<sup>11</sup>

Our connectivity data indeed demonstrate that theta

connectivity is increased when the patient perceives tinnitus in comparison with when he perceives no tinnitus. This suggests that the theta activity might be the carrier wave required for coactivation of the tinnitus network<sup>53,55</sup> and that gamma activity encodes the tinnitus intensity.<sup>61</sup> Our postoperative sLORETA EEG analysis, furthermore, shows a decrease in gamma-band activity in the stimulated secondary auditory cortex associated with a decrease in the perceived tinnitus intensity, demonstrating that this gamma-band activity is indeed causally related to the perceived phantom sound intensity. Combined with the theta functional connectivity changes, this result confirms, by means of EEG, that fMR imaging-guided extradural stimulation interferes with thalamocortical dysrhythmia as previously demonstrated by MEG.<sup>51</sup> It thus suggests that (thalamo)cortical gamma-theta dysrhythmia is a permanent (pathological) state of the normally temporarily present theta-gamma coupling required for normal physiological sensory perception. The BOLD deactivation at the auditory cortex has been shown to be coupled to 5- to 15-Hz local field potentials.<sup>44</sup> The theta (alpha and low beta)-associated BOLD deactivations obtained by tinnitus-matched sound presentation in the imager (Fig. 1B, *green area*) also demonstrate this widespread pattern, in contrast to the gamma-associated BOLD activations, which are limited to the auditory cortex and the ventrolateral prefrontal cortex. When comparing the theta connectivity immediately after implantation to that after 2.5 years of stimulation, we found that the connectivity changes in time. It has been shown that in time the tinnitus network changes,<sup>53</sup> so prolonged stimulation might have the capacity to change functional connectivity as well. This might be of interest, because clinical experience demonstrates that, during the immediate postoperative period, turning on the stimulator immediately suppresses the tinnitus and turning it off immediately (within seconds to minutes) brings it back, demonstrating an absence of residual inhibition. However, after prolonged stimulation (3 years), turning off the stimulator can result in periods of residual inhibition that last for weeks.

## Conclusions

Focal extradural electrical stimulation of the auditory cortex at the area of (thalamo)cortical theta-gamma dysrhythmia is capable of suppressing tinnitus completely. Recordings from the area of BOLD activation on fMR imaging colocalize with gamma and theta peaks on extradural recordings and with decreases of alpha activity. The BOLD activation area also correlates with the electrode poles, which yield maximal tinnitus suppression. These data are in accordance with the thalamocortical dysrhythmia model of tinnitus, at least for the cortical aspect of the model. Our data also suggest that the tinnitus intensity could indeed be encoded by gamma-band activity in the auditory cortex and that the theta activity possibly links the gamma activity to a distributed tinnitus network.

## Disclosure

Educational grants were received from the St. Jude Medical

Neuromodulation Division and the Tinnitus Research Initiative. The first author (D.D.R.) has submitted a patent application for auditory cortex stimulation for tinnitus. The remaining authors report no other conflicts of interest concerning the materials or methods used in this study or the findings specified in this paper.

Author contributions to the study and manuscript preparation include the following. Acquisition of data: Plazier, Kovacs, Sunaert. Critically revising the article: Vanneste. Reviewed final version of the manuscript and approved it for submission: all authors. Statistical analysis: Vanneste, van der Loo, Gais, Kovacs, Sunaert. Administrative/technical/material support: Vanneste.

### Acknowledgments

The authors thank St. Jude Medical Neuromodulation Division and the Tinnitus Research Initiative for their educational grants.

### References

1. Axelsson A, Ringdahl A: Tinnitus—a study of its prevalence and characteristics. **Br J Audiol** **23**:53–62, 1989
2. Barabasi AL, Albert R: Emergence of scaling in random networks. **Science** **286**:509–512, 1999
3. Bartels H, Middel BL, van der Laan BF, Staal MJ, Albers FW: The additive effect of co-occurring anxiety and depression on health status, quality of life and coping strategies in help-seeking tinnitus sufferers. **Ear Hear** **29**:947–956, 2008
4. Boly M, Faymonville ME, Peigneux P, Lambermont B, Damas F, Luxen A, et al: Cerebral processing of auditory and noxious stimuli in severely brain injured patients: differences between VS and MCS. **Neuropsychol Rehabil** **15**:283–289, 2005
5. Boly M, Faymonville ME, Peigneux P, Lambermont B, Damas P, Del Fiore G, et al: Auditory processing in severely brain injured patients: differences between the minimally conscious state and the persistent vegetative state. **Arch Neurol** **61**:233–238, 2004
6. British Society of Audiology: Guidelines on the acoustics of sound field audiometry in clinical audiological applications. 2008 (<http://thebsa.org.uk/docs/Guidelines/soundfieldguidelinesfeb2008.pdf>) [Accessed December 15, 2010]
7. Bullmore E, Sporns O: Complex brain networks: graph theoretical analysis of structural and functional systems. **Nat Rev Neurosci** **10**:186–198, 2009
8. Buzsáki G, Chrobak JJ: Temporal structure in spatially organized neuronal ensembles: a role for interneuronal networks. **Curr Opin Neurobiol** **5**:504–510, 1995
9. Crone NE, Boatman D, Gordon B, Hao L: Induced electrocorticographic gamma activity during auditory perception. **Brazier Award-winning article**, 2001. **Clin Neurophysiol** **112**:565–582, 2001
10. Crönlein T, Langguth B, Geisler P, Hajak G: Tinnitus and insomnia. **Prog Brain Res** **166**:227–233, 2007
11. Csicsvari J, Jamieson B, Wise KD, Buzsáki G: Mechanisms of gamma oscillations in the hippocampus of the behaving rat. **Neuron** **37**:311–322, 2003
12. De Ridder D, De Mulder G, Menovsky T, Sunaert S, Kovacs S: Electrical stimulation of auditory and somatosensory cortices for treatment of tinnitus and pain. **Prog Brain Res** **166**:377–388, 2007
13. De Ridder D, De Mulder G, Verstraeten E, Van der Kelen K, Sunaert S, Smits M, et al: Primary and secondary auditory cortex stimulation for intractable tinnitus. **ORL J Otorhinolaryngol Relat Spec** **68**:48–55, 2006
14. De Ridder D, De Mulder G, Walsh V, Muggleton N, Sunaert S, Möller A: Magnetic and electrical stimulation of the auditory cortex for intractable tinnitus. Case report. **J Neurosurg** **100**:560–564, 2004
15. De Ridder D, van der Loo E, Van der Kelen K, Menovsky T, van de Heyning P, Moller A: Do tonic and burst TMS modulate the lemniscal and extralemniscal system differentially? **Int J Med Sci** **4**:242–246, 2007
16. De Ridder D, van der Loo E, Van der Kelen K, Menovsky T, van de Heyning P, Moller A: Theta, alpha and beta burst transcranial magnetic stimulation: brain modulation in tinnitus. **Int J Med Sci** **4**:237–241, 2007
17. De Ridder D, Vanneste S, van der Loo E, Plazier M, Menovsky T, van de Heyning P: Burst stimulation of the auditory cortex: a new form of neurostimulation for noise-like tinnitus suppression. Clinical article. **J Neurosurg** **112**:1289–1294, 2010
18. De Ridder D, Verstraeten E, Van der Kelen K, De Mulder G, Sunaert S, Verlooy J, et al: Transcranial magnetic stimulation for tinnitus: influence of tinnitus duration on stimulation parameter choice and maximal tinnitus suppression. **Otol Neurotol** **26**:616–619, 2005
19. Dehaene S, Changeux JP, Naccache L, Sackur J, Sergent C: Conscious, preconscious, and subliminal processing: a testable taxonomy. **Trends Cogn Sci** **10**:204–211, 2006
20. Dobie RA: Depression and tinnitus. **Otolaryngol Clin North Am** **36**:383–388, 2003
21. Dobie RA: A review of randomized clinical trials in tinnitus. **Laryngoscope** **109**:1202–1211, 1999
22. Eguíluz VM, Chialvo DR, Cecchi GA, Baliki M, Apkarian AV: Scale-free brain functional networks. **Phys Rev Lett** **94**:018102, 2005
23. Engel AK, Fries P, Singer W: Dynamic predictions: oscillations and synchrony in top-down processing. **Nat Rev Neurosci** **2**:704–716, 2001
24. Friedland DR, Gaggl W, Runge-Samuelson C, Ulmer JL, Koppell BH: Feasibility of auditory cortical stimulation for the treatment of tinnitus. **Otol Neurotol** **28**:1005–1012, 2007
25. Fuchs M, Kastner J, Wagner M, Hawes S, Ebersole JS: A standardized boundary element method volume conductor model. **Clin Neurophysiol** **113**:702–712, 2002
26. Hoffman HJ, Reed GW: Epidemiology of tinnitus, in Snow JB Jr (ed): **Tinnitus: Theory and Management**. Hamilton, Ontario: BC Decker Inc, 2004, pp 16–41
27. Howard DA III: Tinnitus and auditory cortex. **J Neurosurg** **101**:172–172, 2004 (Letter)
28. Jastreboff PJ: Phantom auditory perception (tinnitus): mechanisms of generation and perception. **Neurosci Res** **8**:221–254, 1990
29. Joliot M, Ribary U, Llinás R: Human oscillatory brain activity near 40 Hz coexists with cognitive temporal binding. **Proc Natl Acad Sci U S A** **91**:11748–11751, 1994
30. Jurcak V, Tsuzuki D, Dan I: 10/20, 10/10, and 10/5 systems revisited: their validity as relative head-surface-based positioning systems. **Neuroimage** **34**:1600–1611, 2007
31. Khedr EM, Rothwell JC, Ahmed MA, El-Atar A: Effect of daily repetitive transcranial magnetic stimulation for treatment of tinnitus: comparison of different stimulus frequencies. **J Neurol Neurosurg Psychiatry** **79**:212–215, 2008
32. Kleinjung T, Steffens T, Londero A, Langguth B: Transcranial magnetic stimulation (TMS) for treatment of chronic tinnitus: clinical effects. **Prog Brain Res** **166**:359–367, 2007
33. Kovacs S, Peeters R, Smits M, De Ridder D, Van Hecke P, Sunaert S: Activation of cortical and subcortical auditory structures at 3 T by means of a functional magnetic resonance imaging paradigm suitable for clinical use. **Invest Radiol** **41**:87–96, 2006
34. Laureys S, Faymonville ME, Degueldre C, Fiore GD, Damas P, Lambermont B, et al: Auditory processing in the vegetative state. **Brain** **123**:1589–1601, 2000
35. Llinás R, Ribary U, Contreras D, Pedraarena C: The neuronal basis for consciousness. **Philos Trans R Soc Lond B Biol Sci** **353**:1841–1849, 1998
36. Llinás R, Ribary U, Joliot M, Wang XJ: Content and context in temporal thalamocortical binding, in Buzsáki G, Llinás R,

- Singer W, et al (eds): **Temporal Coding in the Brain**. Berlin: Springer-Verlag, 1994, p 251–272
37. Llinás R, Urbano FJ, Leznik E, Ramírez RR, van Marle HJ: Rhythmic and dysrhythmic thalamocortical dynamics: GABA systems and the edge effect. **Trends Neurosci** **28**:325–333, 2005
38. Llinás RR, Ribary U, Jeanmonod D, Kronberg E, Mitra PP: Thalamocortical dysrhythmia: a neurological and neuropsychiatric syndrome characterized by magnetoencephalography. **Proc Natl Acad Sci U S A** **96**:15222–15227, 1999
39. Londero A, Langguth B, De Ridder D, Bonfils P, Lefaucheur JP: Repetitive transcranial magnetic stimulation (rTMS): a new therapeutic approach in subjective tinnitus? **Neurophysiol Clin** **36**:145–155, 2006
40. Lorenz I, Müller N, Schlee W, Hartmann T, Weisz N: Loss of alpha power is related to increased gamma synchronization—A marker of reduced inhibition in tinnitus? **Neurosci Lett** **453**: 225–228, 2009
41. Mitra PP, Pesaran B: Analysis of dynamic brain imaging data. **Biophys J** **76**:691–708, 1999
42. Møller AR: Similarities between severe tinnitus and chronic pain. **J Am Acad Audiol** **11**:115–124, 2000
43. Mühlhölzer W, Elbert T, Taub E, Flor H: Reorganization of auditory cortex in tinnitus. **Proc Natl Acad Sci U S A** **95**: 10340–10343, 1998
44. Mukamel R, Gelbard H, Arieli A, Hasson U, Fried I, Malach R: Coupling between neuronal firing, field potentials, and fMRI in human auditory cortex. **Science** **309**:951–954, 2005
45. Nir Y, Fisch L, Mukamel R, Gelbard-Sagiv H, Arieli A, Fried I, et al: Coupling between neuronal firing rate, gamma LFP, and BOLD fMRI is related to interneuronal correlations. **Curr Biol** **17**:1275–1285, 2007
46. North RB, Kidd DH, Petrucci L, Dorsi MJ: Spinal cord stimulation electrode design: a prospective, randomized, controlled trial comparing percutaneous with laminectomy electrodes: part II—clinical outcomes. **Neurosurgery** **57**:990–996, 2005
47. Núñez M: Effect of alpha quenching on magnetic field size. **Phys Rev E Stat Nonlin Soft Matter Phys** **63**:056404, 2001
48. Pascual-Marqui RD: Discrete, 3D distributed, linear imaging methods of electric neuronal activity. Part I: exact, zero error localization. 2007 (Abstract) (<http://arxiv.org/abs/0710.3341>) [Accessed December 15, 2010]
49. Pascual-Marqui RD: Instantaneous and lagged measurements of linear and nonlinear dependence between groups of multivariate time series: frequency decomposition. 2007 (Abstract) (<http://arxiv.org/abs/0711.1455>) [Accessed December 15, 2010]
50. Pascual-Marqui RD: Standardized low-resolution brain electromagnetic tomography (sLORETA): technical details. **Methods Find Exp Clin Pharmacol** **24 Suppl D**:5–12, 2002
51. Ramirez RR, Kopell BH, Butson CR, Gaggl W, Friedland DR, Baillet S: Neuromagnetic source imaging of abnormal spontaneous activity in tinnitus patient modulated by electrical cortical stimulation. **Conf Proc IEEE Eng Med Biol Soc** **2009**:1940–1944, 2009
52. Ribary U, Ioannides AA, Singh KD, Hasson R, Bolton JP, Lado F, et al: Magnetic field tomography of coherent thalamocortical 40-Hz oscillations in humans. **Proc Natl Acad Sci U S A** **88**:11037–11041, 1991
53. Schlee W, Hartmann T, Langguth B, Weisz N: Abnormal resting-state cortical coupling in chronic tinnitus. **BMC Neurosci** **10**:11, 2009
54. Schlee W, Mueller N, Hartmann T, Keil J, Lorenz I, Weisz N: Mapping cortical hubs in tinnitus. **BMC Biol** **7**:80, 2009
55. Schlee W, Weisz N, Bertrand O, Hartmann T, Elbert T: Using auditory steady state responses to outline the functional connectivity in the tinnitus brain. **PLoS ONE** **3**:e3720, 2008
56. Seidman MD, Ridder DD, Elisevich K, Bowyer SM, Darrat I, Dria J, et al: Direct electrical stimulation of Heschl's gyrus for tinnitus treatment. **Laryngoscope** **118**:491–500, 2008
57. Smits M, Kovacs S, de Ridder D, Peeters RR, van Hecke P, Sunaert S: Lateralization of functional magnetic resonance imaging (fMRI) activation in the auditory pathway of patients with lateralized tinnitus. **Neuroradiology** **49**:669–679, 2007
58. Steriade M: Grouping of brain rhythms in corticothalamic systems. **Neuroscience** **137**:1087–1106, 2006
59. Tiitinen H, Sinkkonen J, Reinikainen K, Alho K, Lavikainen J, Näätänen R: Selective attention enhances the auditory 40-Hz transient response in humans. **Nature** **364**:59–60, 1993
60. Tonndorf J: The analogy between tinnitus and pain: a suggestion for a physiological basis of chronic tinnitus. **Hear Res** **28**:271–275, 1987
61. van der Loo E, Gais S, Congedo M, Vanneste S, Plazier M, Menovsky T, et al: Tinnitus intensity dependent gamma oscillations of the contralateral auditory cortex. **PLoS ONE** **4**: e7396, 2009
62. Varela F, Lachaux JP, Rodriguez E, Martinerie J: The brainweb: phase synchronization and large-scale integration. **Nat Rev Neurosci** **2**:229–239, 2001
63. Weisz N, Müller S, Schlee W, Dohrmann K, Hartmann T, Elbert T: The neural code of auditory phantom perception. **J Neurosci** **27**:1479–1484, 2007
64. Zöger S, Svedlund J, Holgers KM: The Hospital Anxiety and Depression Scale (HAD) as a screening instrument in tinnitus evaluation. **Int J Audiol** **43**:458–464, 2004

Manuscript submitted March 2, 2010.

Accepted November 15, 2010.

Please include this information when citing this paper: published online January 14, 2011; DOI: 10.3171/2010.11.JNS10335.

Address correspondence to: Dirk De Ridder, M.D., Ph.D., Brai'n, Tinnitus Research Initiative Clinic, and Department of Neurosurgery, University Hospital Antwerp, Wilrijkstraat 10, 2650 Edegem, Belgium. email: [dirk.de.ridder@uza.be](mailto:dirk.de.ridder@uza.be).